Research article

Ink4a/Arf expression is a biomarker of aging

Janakiraman Krishnamurthy,[1] Chad Torrice,[1] Matthew R. Ramsey,[1] Grigoriy I. Kovalev,[2] Khalid Al-Regaiey,[3] Lishan Su,[2] and Norman E. Sharpless[1]

[1]Departments of Medicine and Genetics, and [2]Department of Microbiology and Immunology, The Lineberger Comprehensive Cancer Center, The University of North Carolina School of Medicine, Chapel Hill, North Carolina, USA. [3]Departments of Physiology and Internal Medicine, School of Medicine, Southern Illinois University, Springfield, Illinois, USA.

The *Ink4a/Arf* locus encodes 2 tumor suppressor molecules, p16^{INK4a} and Arf, which are principal mediators of cellular senescence. To study the links between senescence and aging in vivo, we examined *Ink4a/Arf* expression in rodent models of aging. We show that expression of p16^{INK4a} and Arf markedly increases in almost all rodent tissues with advancing age, while there is little or no change in the expression of other related cell cycle inhibitors. The increase in expression is restricted to well-defined compartments within each organ studied and occurs in both epithelial and stromal cells of diverse lineages. The age-associated increase in expression of p16^{INK4a} and Arf is attenuated in the kidney, ovary, and heart by caloric restriction, and this decrease correlates with diminished expression of an in vivo marker of senescence, as well as decreased pathology of those organs. Last, the age-related increase in *Ink4a/Arf* expression can be independently attributed to the expression of *Ets-1*, a known p16^{INK4a} transcriptional activator, as well as unknown *Ink4a/Arf* coregulatory molecules. These data suggest that expression of the *Ink4a/Arf* tumor suppressor locus is a robust biomarker, and possible effector, of mammalian aging.

Introduction

Aging is a complex set of phenotypes characterized by reduced repair and/or regeneration of lost or damaged cells. Although studies in lower organisms have linked metabolism and the production of oxygen radicals with the rate of aging (reviewed in ref. 1), less is known about the molecular effectors of aging in mammals. As opposed to homeostasis in organisms with a postmitotic soma, such as *Drosophila* and *Caenorhabditis elegans*, mammalian homeostasis depends on the persistent and obligate function of reservoirs of self-renewing tissue stem cells that are necessary for tissue regeneration. Therefore, regulators of stem cell longevity are thought to play a role in human aging (reviewed in ref. 2). In particular, mediators of senescence, an important tumor suppressor mechanism and specialized form of growth arrest, have been suggested to play a role in aging by limiting the long-term growth of these self-renewing compartments (reviewed in refs. 3, 4). For example, excess activity of p53 has been shown to induce premature aging in mice in multiple tissue types (5, 6). For these reasons, it has been argued that some aspects of aging may result from the beneficial, anticancer functions of mediators of senescence such as p53, ARF, and p16^{INK4a}.

We sought to examine the role of p16^{INK4a}, ARF, and related cell cycle inhibitors in mammalian aging. This choice was motivated by the importance of p16^{INK4a} and/or ARF in the senescence in vitro of many murine and human cell types, e.g., islets (7), fibroblasts (8, 9), keratinocytes (10, 11), and macrophages (12); the fact that expression of p16^{INK4a} significantly accumulates with normal aging in rodents and humans in a variety of tissues (13–19); and the fact that p16^{INK4a} and Arf appear to be principal mediators of stem cell

longevity in vivo (20–24). Toward this end, we sought to define the pattern of expression of cell cycle inhibitors in aging rodents, and to determine the effects of known regulators of aging such as caloric restriction on the expression of these inhibitors of proliferation.

Results

Expression of Ink4a/Arf in vivo. We determined the expression of cyclin-dependent kinase inhibitor (CDKI) family members, which are principal regulators of the mammalian cell cycle (25). CDKIs inhibit the kinase activity of Cdk2, Cdk4, and Cdk6, thereby inhibiting phosphorylation of their target protein Rb and eliciting G1 arrest. Eighteen quantitative real-time PCR strategies (Supplemental Table 1; supplemental material available at http://www.jci. org/cgi/content/full/114/9/1299/DC1) were used to assay CDKI expression in tissues from old and young syngeneic adult rodents (Figure 1, A and B). We also tested the expression of Arf, a cell cycle inhibitor through its regulation of p53 stability, because Arf is coregulated with p16^{INK4a} (Figure 1, A and B), and its expression has previously been shown to increase with aging in the mouse (18).

A marked increase (3-fold or greater) in the expression of *p16^{INK4a}* was seen in 26 of 27 organs analyzed from 15 murine and 12 rat tissues. Particularly large (>30-fold) increases in relative terms of the ratio of RNA expression in old versus young tissues (old/young ratio) were seen in the murine cecum, kidney, ovary, and uterus (Figure 1A; log$_2$ scale), while the highest expression in absolute terms was seen in lung, lymph node, adrenal, and uterus from aged animals (Figure 1B; log$_{10}$ scale). The geometric mean of the old/young ratios among the 15 murine tissues analyzed was 9.7 (i.e., the average tissue demonstrated an approximately 10-fold increase in the expression of *p16^{INK4a}* with aging). This value is likely an underestimate of the true average fold increase, because in tissues such as the pancreas and bone marrow (Figure 1A), *p16^{INK4a}* expression was below the level of detection in young animals. Therefore, in these tissues, only a minimum estimate of the fold increase in expression in these tissues could be determined. Similarly, *Arf* expression increased severalfold in most of the tissues examined, particularly heart, duodenum, kidney, and uterus (Figure 1, A and B). The geo-
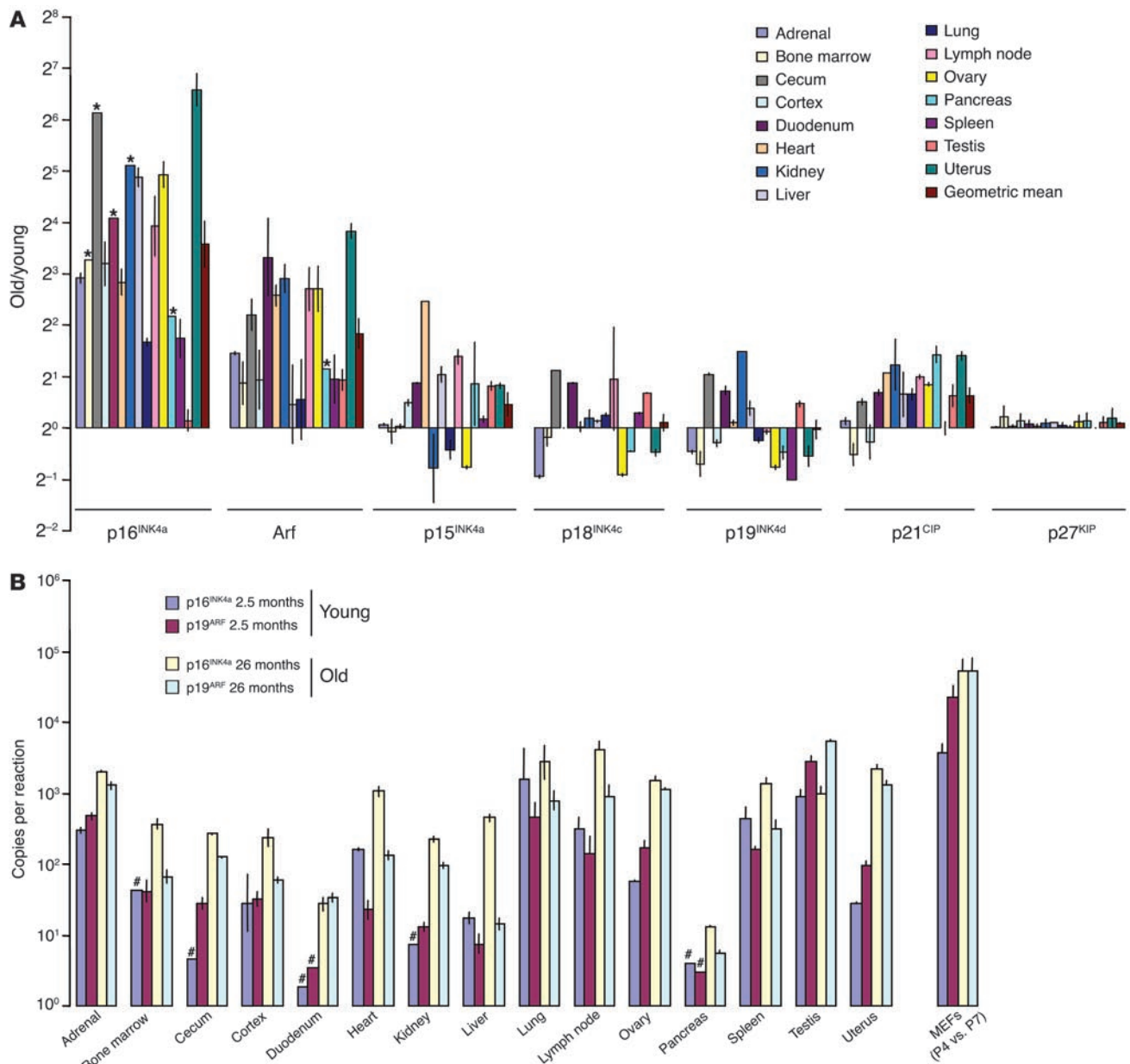
Figure 1
Expression of the *Ink4a/Arf* locus increases with aging. (**A**) Relative expression. The ratios (log₂ scale) of the expression of cell cycle inhibitors — old (26 months)/young (2.5 months) — from 15 tissues is graphed ± SEM. Each estimate represents the mean of 8–32 quantitative RT-PCR reactions on independent RNA samples derived from 4–6 mice. *Minimum estimate of old/young ratio. (**B**) Absolute expression. The absolute copy number of *p16^INK4a* and *Arf* mRNA molecules (log₁₀ scale) per 90 ng total RNA RT-PCR from 15 tissues of young (2.5 months) and old (26 months) mice is graphed ± SEM. Murine embryo fibroblasts (MEFs) at early (P4) and late (P7) passage are shown for comparison. #Maximum estimated expression is indicated, as expression was below the level of detection.

metric mean of the *Arf* old/young ratios was a 3.5-fold increase, while the next highest cell cycle inhibitor, p21^CIP, demonstrated only a 1.4-fold average increase. These data do not exclude a specific role for another CDKI in a particular tissue; for example, *p15^INK4b* showed an approximately 5-fold increase in expression in the heart with aging. Likewise, our data do not exclude the possibility that certain of the CDKIs (e.g., p18^INK4c [ref. 26] or p27^KIP [ref. 27]) are regulated predominantly in a posttranscriptional manner with aging. Nonetheless, *Ink4a/Arf* upregulation appears to be a strong correlate to

organismal aging across many tissue types, and this marked and widespread upregulation is unique among the major in vivo inhibitors of the mammalian cell cycle.

In terms of absolute transcript number and protein expression, the expression of p16^INK4a and Arf was considerably lower in tissues from aged mice than in primary cultures of murine embryo fibroblasts (Figure 1B), even at passage 4 (less than 14 days in vitro). This observation emphasizes that the act of culture itself potently induces the *Ink4a/Arf* locus (28) but also suggests that in vivo *Ink4a/Arf*
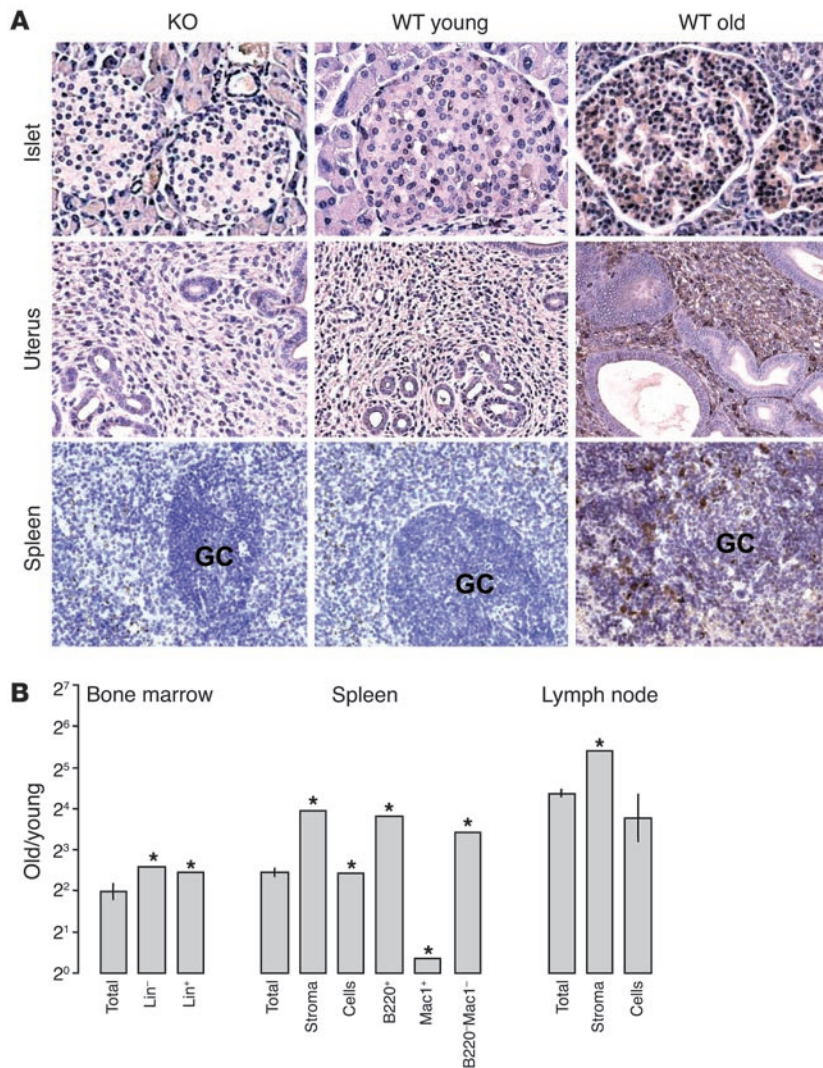
Figure 2
p16[INK4a] expression in specific compartments by immunohistochemistry and cell purification. (**A**) Immunoperoxidase staining performed on paraffin-embedded sections of germ-line *p16[INK4a]*-deficient (KO), WT young (3.5 months), and WT old (25 months) murine tissues using an anti-p16[INK4a] antibody. Positively staining cells demonstrate both nuclear and cytoplasmic expression. GC, germinal center. (**B**) Relative expression ratios (old/young, $\log_2$ scale) of *p16[INK4a]* in specific compartments (average purity >94% for all fractions) of bone marrow (lin⁻, 2%; lin⁺, 97%), spleen (B220⁺, 48%; Mac1⁺, 9%; B220⁻Mac1⁻, 22%), and lymph node. Asterisks indicate that *p16[INK4a]* expression was undetectable in these cell populations from young mice, and therefore a minimum estimate of the fold increase is shown.

expression increases only in a relatively small subset of cells within a given tissue (e.g., the β cells of the pancreas; Figure 2A and ref. 17). To determine in which organ compartments the expression of *Ink4a/Arf* increased, we performed additional lines of analysis including immunohistochemistry (IHC) and mRNA quantification in purified populations of sorted cells (Figure 2, A and B, and data not shown). Using these approaches, we were able to define the compartmental expression of p16[INK4a] and/or Arf in selected tissues from aging rodents (summarized in Table 1).

This analysis led to several conclusions. First, there was a good correlation in most tissues between mRNA expression and protein expression. An exception, however, was the lung, where RNA expression of *p16[INK4a]* even from young mice was higher in absolute terms than in several tissues from old mice (Figure 1B) yet protein expression was not detected by IHC or immunoprecipitation–Western analysis (not shown). This result could be attributable to either translational regulation of p16[INK4a] (29) or decreased protein stability in this tissue. Furthermore, we detected p16[INK4a] expression in a variety of cell types, including lining epithelium (e.g., of the renal cortex), mesenchyme (of the uterus), lymphocytes (in the spleen and lymph nodes), and specialized endocrine secretory tissues (e.g., pancreatic islet and adrenal) (Figure 2, A

and B; Table 1). For example, in the uterus, there was marked expression of p16[INK4a] in the stroma of aged mice, but less so by IHC in the uterine epithelium. In the kidney, a marked increase in expression was noted in the cortical tubules, with detectable, but significantly less, expression in the medulla and glomeruli. In the spleen, increased expression of p16[INK4a] in both the stromal (red pulp) and lymphocyte (white pulp) compartments was noted, although this was higher in stroma (Figure 2, A and B). In aggregate, these data suggest that the expression of *p16[INK4a]* mRNA and protein increases in cells of varied histogenetic origins with aging. These results indicate that expression of the *Ink4a/Arf* locus can be induced in many if not most cell types in vivo, as would be suggested by related in vitro observations (7–12), as well as by the locus's role in the suppression of a wide variety of cancer types (30).

To permit quantification of the compartmental expression of *p16[INK4a]*, hematopoietic organs were harvested and specific cell types purified (Figure 2B). Expression of *p16[INK4a]* increased with aging in both the stromal and the cellular (predominantly T cell) compartments of lymph nodes, but to a greater degree in the stroma (42-fold vs. 13-fold). Similarly, both the stromal and cellular compartments of the spleen showed increased expression of *p16[INK4a]* with aging (15-fold vs. 5-fold). Among the splenic cellular elements, the predominant increases were seen in lymphocytes (B220⁺, 48% of total splenic cells) and cells that did not express B lymphocyte or myeloid markers (double negative for Mac1 and B220, 22% of cells), whereas little increase was seen in the myeloid compartment (Mac1⁺, 9% of cells). Lastly, we compared the expression of *p16[INK4a]* and *Arf* in lineage-negative (2%) versus lineage-positive (98%) bone marrow cells. In this compartment, the principal increase in expression was in lineage-negative cells, which are enriched for hematopoietic stem and progenitor cells (HSPCs) (31). This finding is consistent with the reported role of *Ink4a/Arf* expression in HSPCs and early committed progenitors from adult mice (21). Therefore, *Ink4a/Arf* can be expressed in several cell types of hematopoietic organs, including stromal elements, lymphocytes, and progenitor cells.

Table 1

Expression of p16[INK4a] in murine tissues (present work) as compared with published human IHC data

Tissue	Fold increase	Abs. exp. in old organ[A]	mRNA expression (by sorting or in situ)	IHC in mouse (present work)	IHC in human (ref.)
Adrenal	7.6	2,027	ND	ND	ND
Bone marrow	>9.7	366	+++ Lin⁻ cells, ++ Lin⁺ cells	ND	Rare + macrophages, plasma cells (17)
Cecum	>70.2	267	ND	ND	Not detected (17)
Cortex	9.2	235	ND	ND	Not detected (17)
Duod.	>17.0	27	ND	ND	ND
Heart	7.2	1,064	Not detected	ND	Myocardium (63)
Kidney	>34.5	220	ND	+++ Cortical tubules; tr. glomeruli	Cortical tubules, rare glomeruli (13, 16)
Liver	29.4	447	ND	ND	Not detected (17)
Lung	3.2	2,714	+++ Small bronchi, + alveoli	Not detected	Rare + alveolar cells (17)
Lymph node	15.3	4,146	++++ Stroma, +++ lymphocytes	ND	ND
Ovary	30.5	1,514	ND	+++ Stroma	Not detected (17)
Panc.	>4.5	11	ND	Islets	Islets (17)
Spleen	3.3	1,357	++++ Stroma, ++ lymphocytes	++++ Stroma, ++ lymphocytes	Stroma (17)
Testis	1.1	976	+ Leydig cells, +++ epididymis	ND in mouse; Leydig cells in rat	Epididymis (17)
Uterus	96.0	2,140	++ Stroma and epithelium	++++ Stroma, tr. epithelium	Epithelium and stroma (17)

Abs. exp., absolute expression; ND, not determined; Duod., duodenum; Panc., pancreas; tr., trace. [A]Copies per 90 ng total RNA.

Caloric restriction retards p16^INK4a accumulation. Caloric restriction (CR) retards aging in many species, but the molecular effectors of this are unknown (32). To examine the effects of CR on *p16^INK4a* expression, we harvested total RNA from organs from calorically restricted (CR) and ad libitum–fed (AL) Fischer 344 (F344) rats (Supplemental Figure 1, A and B) (33). We confirmed that *Ink4a/Arf* expression increased with aging in 12 different tissues from AL rats (representative data shown in Figure 3A). There was excellent concordance in the fold increase of *Ink4a/Arf* and *p21^CIP* expression between mouse and rat tissues from AL animals, except in the testis. In murine testis, no increase in *p16^INK4a* was seen (Figure 1, A and B), whereas in rat testis, a greater-than-135-fold increase in *p16^INK4a* expression was noted (Figure 3A). A histologic examination of rat testis from old AL males, however, demonstrated marked involvement with Leydig cell tumor (Supplemental Figure 1C), which occurs spontaneously in the majority of AL F344 rats greater than 24 months of age (34), and which highly expresses *p16^INK4a* (not shown). Increases in Arf expression similar in magnitude to those in the mouse were also noted across this panel of tissues, as were more modest increases in *p21^CIP* (Figure 3A). Therefore, mice and rats appear to age similarly with respect to *Ink4a/Arf* expression.

When compared with tissues from AL animals, several, but not all, tissues from CR animals showed marked reductions in the age-induced increase of *Ink4a/Arf* expression. A 2- to 16-fold attenuation in the age-induced expression of *p16^INK4a* was seen in adrenal, heart, kidney, ovary, and testis; but CR did not attenuate *Ink4a/Arf* expression in the lung, lymph node, spleen, and liver (Figure 3A). Unexpectedly, in the uterus, CR appeared to induce a significant *increase* in *Ink4a/Arf* expression with aging. Consistent with a previous report (34), we noted that aged CR males demonstrated greatly reduced Leydig cell hyperplasia (Supplemental Figure 1C) compared with AL animals. Correspondingly, this decreased tumor burden correlated with a marked reduction in the age-induced increase in *p16^INK4a* expression (135-fold in AL rats vs. 58-fold in CR rats). Therefore, the decrease in *p16^INK4a* expression with CR in aged rat testis likely results from an antineoplastic effect of CR. In contrast, the marked decrease in *p16^INK4a* expression in the cortical tubules of the kidney (Figure 3B) from CR animals correlated with decreased nephritis (not shown), a chronic disease seen with nearly complete penetrance in aged F344 rats and a principal limit to the longevity of this strain (34). Therefore, in both of these tissues, the decrease in *Ink4a/Arf* expression occurred in concert with a CR-induced reduction of a disease state, suggesting that increased *Ink4a/Arf* expression in some circumstances may predispose to organ pathology, presaging organ failure and death. These observations also predict that tissue-specific increases in *Ink4a/Arf* expression with aging likely will vary among mammals (and even across inbred strains of rodents) to reflect specific predispositions to disease resulting from unshared genetics and/or environmental exposures.

We also tested the relationship of *Ink4a/Arf* expression with other aging models. Several single-gene mutations that decrease IGF-1 extend longevity (reviewed in ref. 35), through a mechanism that appears at least partially distinct from CR (36). We tested *Ink4a/Arf* expression in both lung and kidney from old and young growth hormone receptor⁺/⁺ (GHR⁺/⁺) and GHR⁻/⁻ mice (37) that had been fed ad libitum or CR diets. The age-induced expression of *Ink4a/Arf* in mice from this cohort of mixed genetic background was more heterogeneous than in either the inbred F344 rat or the C57BL/6 mouse cohort (Supplemental Figure 2). Nonetheless, in accord with our observations in the rat, CR significantly reduced *p16^INK4a* and *Arf* expression in the murine kidney (Supplemental Figure 2). GHR deficiency, however, had no effect on *p16^INK4a* or *Arf* expression in the kidney, although modest reductions in *p16^INK4a* and *Arf* expression were noted in the lung from GHR-deficient animals (Supplemental Figure 2). These results confirm in another species the effect of CR on *Ink4a/Arf* expression in the kidney and also suggest that GHR deficiency and CR enhance longevity by molecularly distinct mechanisms in distinct tissues, as has been suggested by other methodologies (36, 38).

Furthermore, we sought to determine the functional significance of *Ink4a/Arf* expression in aging mammals. We used a well-
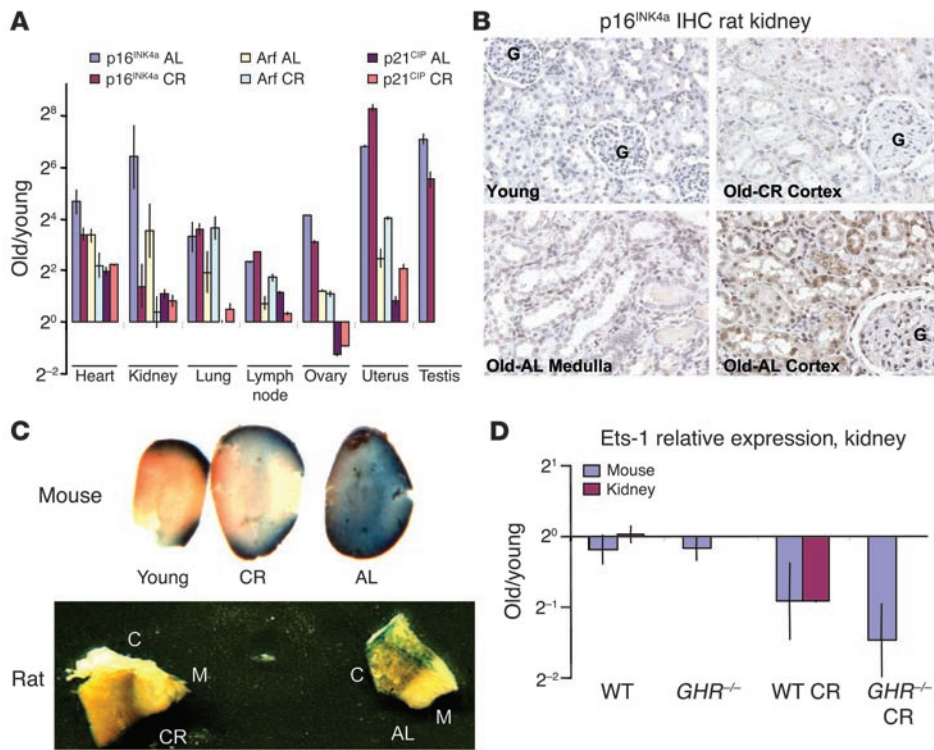
Figure 3
Effects of caloric restriction and GHR deficiency on gene expression and aging. (**A**) Relative expression ratios (old/young, $\log_2$ scale) of cell cycle inhibitors in 7 tissues derived from old (28 months) and young (3 months) AL or CR F344 rats. The relative ratios are graphed ± SEM. Each estimate represents the mean of 8–16 quantitative RT-PCR reactions on independent RNA samples derived from 4 rats. (**B**) Immunoperoxidase staining on paraffin-embedded kidney sections from young, old AL, and old CR F344 rats using an anti-p16^{INK4a} antibody. G, glomeruli seen in cortical sections. (**C**) SA-β-gal staining in AL and CR mouse and rat kidney. C, renal cortex; M, renal medulla. Thin tissue slices were stained for mice, as opposed to small tissue wedges for rats. SA-β-gal activity is predominantly restricted to the renal cortex. (**D**) Relative expression ratios (old/young, $\log_2$ scale) of *Ets-1* in kidneys derived from AL and CR rats and mice. Results from the kidneys from AL and CR mice with and without GHR deficiency are also shown. Each estimate represents the mean of 8–32 quantitative RT-PCR reactions on independent RNA samples derived from 8 mice or 4 rats.

locus (43) (Supplemental Figure 3). The expression of these genes was determined across multiple tissues from young and old mice and/or rats, with and without CR. We calculated Pearson correlation coefficients of the log-transformed old/young ratios of all genes across the tissue types analyzed. As expected, we found a high correlation between *p16^{INK4a}* and *Arf* expression ($r = 0.75$, $P < 0.0001$) and a modest correlation between *Arf* and *p21^{CIP}* ($r = 0.37$, $P = 0.03$), but no significant correlation between *p16^{INK4a}* and *p21^{CIP}*. These results are consistent with the known transcriptional relationships of these genes; in particular, several proteins (43–47) have been identified that coordinately regulate the expression of both *Ink4a/Arf* products, and Arf regulates p53 activity, which in turn induces p21^{CIP} expression. Unexpectedly, we found a high correlation between *p18^{INK4c}* and *p19^{INK4d}* ($r = 0.68$, $P = 0.002$), which suggests that these genes are regulated by common or related transcriptional elements. Although these homologous INK4s are concomitantly expressed in many tissues (18), we are not aware of previous data showing coordinated expression in vivo.

The expression of *Ink4a/Arf* regulators was next considered (Supplemental Figure 3). A weak negative correlation was found between the expression of *Id1* and that of *p16^{INK4a}* ($r = -0.40$, $P = 0.07$), consistent with Id1's known role as a transcriptional repressor of p16^{INK4a} (40, 42). No significant correlation was seen between *Bmi-1* expression and that of either *p16^{INK4a}* or *Arf* (not shown). Remarkably, however, a strong correlation was noted between p16^{INK4a} and *Ets-1* ($r = 0.62$, $P < 0.001$; Figure 4A), but not between *Arf* and *Ets-1* ($r = 0.15$, $P = 0.40$). This observation is consistent with the finding that Ets-1 induces the expression of *p16^{INK4a}*, but not *Arf*, in cultured cells (40, 41) and suggests that a significant component of the in vivo variance in *p16^{INK4a}* expression with aging ($r^2 = 0.38$) results from transcriptional activation by Ets-1 (Figure 4B). Moreover, a reduction in *Ets-1* expression was seen in the kidney of CR rats and mice (Figure 3D), which suggests that increased metabolism is upstream of Ets-1 activation in the aging kidney. Similarly, the strong correlation between *p16^{INK4a}* and *Arf* also suggests that an unknown coregulator(s) of *p16^{INK4a}* and *Arf* exerts a powerful effect ($r^2 = 0.49$) on the expression of both *Ink4a/Arf* products with aging, and that this coregulator(s) must be independent of Ets-1 (as *Arf* and *Ets-1* are not correlated). Therefore, the in vivo expression of *p16^{INK4a}* in aging appears to reflect almost equally
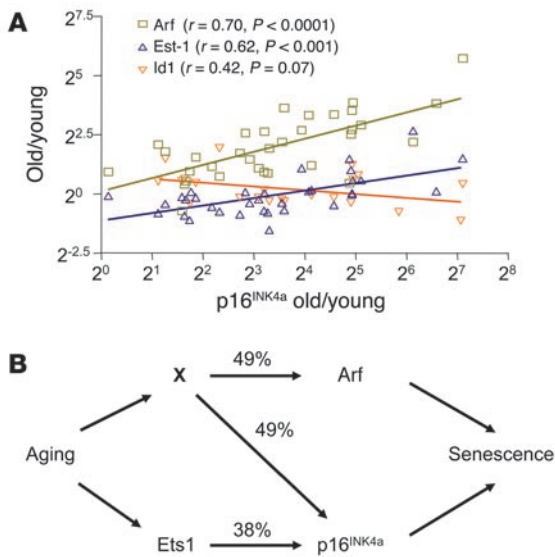
described in vivo marker of senescence, senescence-associated β-galactosidase (SA-β-gal) expression, a high-pH galactosidase activity detectable in senescent cells and tissues (39). This assay was limited in most tissues (e.g., liver and spleen) because of high background activity but was interpretable in both murine and rat kidney (Figure 3C), in accord with a previous report (15). A significant increase in SA-β-gal activity was detected in aging kidney from AL mice and rats (Figure 3C) and was predominantly restricted to the renal cortex, a pattern of expression that overlapped with p16^{INK4a} expression. This increase in SA-β-gal activity was, like the increase in p16^{INK4a} expression, abolished by CR, which suggests that *Ink4a/Arf*–induced senescence is induced in the renal cortex as a result of increased metabolism.

Ets-1 and a common Ink4a/Arf regulator modulate p16^{INK4a} expression with aging. In an effort to determine the factors responsible for the marked accumulation of *Ink4a/Arf* with aging, we next determined the expression of 3 principal regulators of *Ink4a/Arf* expression: Ets-1, an activator of *p16^{INK4a}* (40, 41); Id1, a transcriptional repressor of *p16^{INK4a}* (40, 42); and Bmi-1, a repressor of the *Ink4a/Arf*

Figure 4
p16^INK4a expression with aging strongly correlates with *Arf* and *Ets-1* expression. (**A**) A scatter plot (log₂ scale, both axes) of the ratios (old/young) of *p16^INK4a* expression versus the expression ratios (old/young) of *Arf*, *Ets-1*, and *Id1* seen in the corresponding tissue (*n* = 22–70 data pairs per gene from up to 15 tissues in both mouse and rat). Each ratio represents a mean value of multiple measurements per tissue as described in Methods. A best-fit line determined by linear regression is shown for each data series, with Pearson correlation coefficient and 2-tailed *P* value. No significant correlation was seen between *Arf* and *Ets-1*, or between *Arf* or *p16^INK4a* and *Bmi-1* (not shown). (**B**) Arrows show known or inferred transcriptional relationships, and numbers indicate the covariances (r^2) for the linked elements as determined in **A**. As *p16^INK4a* and *Arf* do not regulate one another, it seems reasonable to assume that an unknown coregulator (X) modulates the expression of both transcripts with aging, explaining their strong correlation (r^2 = 48%). Furthermore, as *Arf* and *Ets-1* do not covary, X and Ets-1 must be independent. X need not represent a single transcription factor: it may represent the combined activity of several genes (e.g., the PcG family members) or genes that affect other transcript properties, such as message stability. This model suggests that the majority (87%) of the variance in *p16^INK4a* expression with aging in the analyzed tissues can be attributed to the activity of X and Ets-1.

a *p16^INK4a*-specific effect that correlates with *Ets-1* expression, and an independent, *Ink4a/Arf* coregulatory effect.

Discussion
This work adds to a growing body of evidence suggesting that in vivo senescence, induced by *Ink4a/Arf* expression, plays a causal role in the aging of certain tissue types. First, as shown in this work, *Ink4a/Arf* expression is not only tightly linked with aging but is influenced by CR and correlates with SA-β-gal expression. *Ink4a/Arf* expression has also been shown to increase in several tissues in a murine model of premature aging (48), and expression of *p16^INK4a* or *Ink4a/Arf* correlates in vivo with impaired proliferation and failure of hematopoietic stem cells (20, 21, 23, 24). While the functional consequences of *Ink4a/Arf* expression in aging tissues are an area of active investigation, *p16^INK4a* deficiency has been shown to ameliorate an age-related decline in T cell responsiveness to CD3 and CD28 (49), a hallmark of aging in the murine immune system (50). Similarly, neural stem cells from *Bmi-1*–deficient ani-

mals demonstrate increased *Ink4a/Arf* expression and impaired regenerative potential; and this phenotype can be partially rescued by *p16^INK4a* deficiency (22). In aggregate, these results suggest that *p16^INK4a* and/or *Arf* expression is not merely a biomarker, but also an *effector*, of aging, presumably by limiting the self-renewal capacity of disparate tissues including at least lymphoid organs, bone marrow, and brain. Further determination of the functional role of the *Ink4a/Arf* locus in other aging tissues, as well as the relative contribution p16^INK4a versus Arf, will require further study of mice with germ-line and tissue-specific deletion of p16^INK4a and/or Arf.

We detected a significant attenuation of age-induced *Ink4a/Arf* expression by CR in several tissues, but particularly in the kidney, where the effect was nearly complete. The reduction in *Ink4a/Arf* expression correlated with decreased nephritis in aged F344 rats, a major limit of longevity in this strain (34). Therefore, it is tempting to speculate that *Ink4a/Arf* expression limits the ability of aged kidney to self-repair, resulting in organ failure and death. Our analysis of tissue from GHR-deficient animals was too limited to determine the effects, at the organismal level, of GHR deficiency on *Ink4a/Arf* expression; but in contrast to CR, GHR loss was not seen to affect p16^INK4a expression in the aging kidney (Supplemental Figure 2). It is possible that reductions in IGF-1 similarly retard the increase in *Ink4a/Arf* expression in other tissues; this would explain the ability of CR to extend the longevity of IGF-1–deficient animals (36). Alternatively, IGF-1 deficiency may work through a distinct, *Ink4a/Arf*–independent mechanism to retard aging.

As rodents have large telomeres and promiscuously express telomerase (51, 52), the signal that induces *Ink4a/Arf*–mediated senescence in the kidney and other organs is not likely to be telomere-based. We were, however, able to demonstrate a strong correlation between *Ets-1* expression and *p16^INK4a* expression with aging across 27 different tissues from 2 species, with and without CR. Given that Ets-1 is a direct transcriptional activator of *p16^INK4a* in vitro (40, 41), these data suggest that Ets-1 is a principal determinant of *p16^INK4a* expression with aging in vivo. Ets-1, in turn, is regulated by a variety of stress-related signals and, in particular, MAPK activity. Ets-1 activation has been linked to both ERK (53, 54) and p38^MAPK (55) signaling, while recent genetic evidence has shown that p38^MAPK activation is associated with increased *Ink4a/Arf* expression in vivo (56). These observations are consistent with the model (Figure 4B) that presently unidentified stresses activate Ets-1 via MAPK pathways to induce a p16^INK4a-mediated senescence in aging organisms.

By statistical methods, we additionally inferred the existence of an unknown coregulatory factor(s) that is distinct from Ets-1 and that modulates the expression of both *p16^INK4a* and *Arf* with aging. An obvious candidate is the Polycomb group (PcG) protein Bmi-1, which has been shown to regulate *p16^INK4a* and *Arf* expression in stem cells in vivo (20–22, 57). We did not, however, detect a negative correlation between *Bmi-1* expression and either *p16^INK4a* or *Arf* in most aging tissues. Therefore, transcription of *Bmi-1* is not likely to be a predominant regulatory mechanism of *Ink4a/Arf* expression in vivo across multiple tissue types, but this analysis does not exclude a specific role for Bmi-1 in a particular tissue. Along these lines, we detected greater-than-2-fold decreases in *Bmi-1* expression with aging in spleen and bone marrow (Supplemental Figure 3), which suggests that perhaps Bmi-1–containing PcG complexes are of particular importance in repressing *Ink4a/Arf* expression in hematopoietic tissues, as has been suggested (20, 21, 43). Likewise, it is possible that related

Ink4a/Arf–repressing PcG family members such as Cbx7 (58) or Mel18 (59) subsume the function of Bmi-1 in other tissues; that PcG complex activity is regulated post-transcriptionally; or that unidentified non-PcG molecules are important coregulators of *Ink4a/Arf*. In this regard, it will also be of future interest to determine the links, if any, between *Ink4a/Arf* expression and known regulators of aging such as Foxo proteins and SirT1 (60, 61).

A molecular biomarker of physiologic, as opposed to chronologic, age is needed in clinical medicine. While other molecular markers of aging have been suggested, we believe the analysis of *INK4a/ARF* expression may prove particularly fruitful in this regard, for several reasons. First, the change in p16[INK4a] expression with aging is large — over 10-fold in many tissues — and relatively simple to measure by either immunohistochemical methods or quantitative real-time PCR analysis. For example, there is a clinically validated, commercially available kit (DakoCytomation Inc.) for use in the detection of p16[INK4a] expression, and many anatomic pathologists are already comfortable with the interpretation of p16[INK4a] IHC. Moreover, our results demonstrate that *Ink4a/Arf* can be expressed in many cell types in response to age-induced stresses, and that *Ink4a/Arf* expression changes in at least a subcompartment of the majority of mammalian organs with aging. For this reason, p16[INK4a] or ARF expression may be a particularly robust marker of aging, useful for the study of many cell types in disparate organs. Lastly, given the probable causal role of p16[INK4a] and/or ARF in aging, expression of *INK4a/ARF* should be a stronger correlate of aging than expression of other genes whose expression is merely epiphenomenal.

One anticipates that a well-defined molecular marker of aging could be used for at least 4 clinical purposes: (a) to facilitate the forecasting of disease progression in premorbid syndromes such as renal insufficiency and cardiomyopathy; (b) to provide a surrogate marker for efficacy of anti-aging therapeutics; (c) to predict future toxicity from noxious therapies such as chemo- or radiotherapy and surgery that require tissue regeneration and repair; and (d) to determine donor suitability for bone marrow, solid organ, and tissue allografts. The utility of *INK4a/ARF* expression in predicting, and perhaps determining, a tissue's future regenerative potential — i.e., indications (c) and (d) above — is a topic of active, ongoing study. This work, however, does serve as "proof of principle" for the use of *Ink4a/Arf* expression for indications (a) and (b): we demonstrate that *Ink4a/Arf* expression correlates with tissue aging and alterations in disease progression in the rodent kidney and testis, and that reduced expression of the locus correlates with response to an anti-aging therapy, caloric restriction. Therefore, our data suggest that the measurement of *INK4a/ARF* expression may similarly be of clinical benefit in the determination of human physiologic age.

Methods

Animals. All animals were housed and treated in accordance with protocols approved by the institutional care and use committee for animal research at the University of North Carolina. All murine analyses were performed in C57BL/6 mice unless otherwise mentioned. For cell sorting experiments, 22- to 25-month-old mice of mixed genetic background (C57BL/6 × NIH Black Swiss; from Yue Xiong, University of North Carolina) were analyzed. Old (21 months) and young (5 months) GHR KO and WT (CR and AL) mice of mixed genetic background (derived from Ola-BALB/c, C57BL/6, and C3H; courtesy of John Kopchick, Ohio University, Athens, Ohio, USA) were analyzed. CR for this murine cohort was done as previously described (38). Aged rodents were obtained from the aged-rodent colonies of the National Institute on Aging (ref. 33; see also http://www.nia.nih.

gov/research/rodent.htm) and euthanized at our facility, and organs were harvested as described below. For murine studies, old (25–26 months) and young (2.5–3.5 months) C57BL/6 mice (3 males and 3 females) were analyzed. For CR experiments, old (28 months) and young (3 months) F344 AL rats (2 old and 2 young males, 2 old and 2 young females) were obtained, as well as old (28 months) CR littermates (2 males and 2 females).

Animals were euthanized by CO_2 inhalation, and organs were harvested. Organs were grossly dissected free of contaminating tissue (e.g., adipose) and then snap-frozen. RNA was harvested from a matched portion of the organ (e.g., the superior half of the kidney) in all instances to assure that results did not differ because of organ composition. For RNA analysis, tissues were collected after cardiac perfusion with RNA*later* (Ambion Inc.) or after snap-freezing in liquid nitrogen. For IHC and H&E staining, organs were harvested and fixed as described below, and then stored in 70% ethanol until paraffin embedding.

Quantitative real-time PCR. Total RNA was extracted from tissues, serially passaged murine embryo fibroblasts (each passage corresponds to 3 days in vitro), or sorted cell samples using a QIAGEN RNeasy RNA isolation kit according to the manufacturer's instructions. Transcription into cDNA was done in a 20-µl volume using oligo-dT$_{(12-18)}$ or random hexamer and ImProm-II reverse transcriptase (Promega Corp.) according to the manufacturer's instructions. All PCR reactions were carried out in a final volume of 20 µl and were performed in duplicate for each cDNA sample in the ABI PRISM 7700 Sequence Detection System (Applied Biosystems) according to the manufacturer's protocol. All experiments were done on organs from at least 2 different animals in each group (old vs. young, CR vs. AL).

Sequence-specific primers and probe were designed using Primer Express (Applied Biosystems) for the indicated genes (Supplemental Table 1). Oligonucleotide primers and probes were synthesized by MWG Biotech. All primer sets were designed to span an intron. Predeveloped assays were purchased from Applied Biosystems for the additionally listed murine and rat genes (Supplemental Table 1). The reaction mix consisted of Universal Master Mix No AmpErase UNG (Applied Biosystems), 0.25 µM fluorogenic probe, 0.9 µM of each specific forward and reverse primer, and 9 µl of diluted cDNA (equivalent to ~90 ng total RNA). Amplifications were done under standard conditions. The number of PCR cycles needed to reach the fluorescence threshold was determined in duplicate for each cDNA, averaged, and then normalized to at least 1 reference gene (18S, GAPDH, or TATA-binding protein [TBP]; see Supplemental Figure 4 for further details) to yield the cycle number at which fluorescence threshold was reached (C_t). The ratio of expression in old versus young tissues (old/young) was determined as $2^{[C_t(\text{old}) - C_t(\text{young})]}$; therefore, $\log_2(\text{old/young}) = C_t(\text{old}) - C_t(\text{young})$. Ratios were log-transformed for calculations of SE and Pearson correlation coefficients using Prism software (GraphPad Software Inc.). For absolute quantification of transcript copy number for p16[INK4a], p15[INK4b], p19[ARF], p21[CIP], p18[INK4c], and p19[INK4d], the fragment of interest was cloned and a standard curve generated with serial 4-fold dilutions (Supplemental Figure 5). For all assays tested, the PCR reaction was linear over the range studied (19–40 cycles of amplification; Supplemental Figure 5). If C_t was not reached by 40 cycles, expression was considered below the limit of detection. All RT-PCR reactions gave a single band when analyzed by gel electrophoresis, and all reactions used a fluorochrome-labeled internal probe to enhance sensitivity and specificity.

Cell sorting of bone marrow, lymph node, thymus, and spleen. Tissues from 5- and 22-month old mice (*n* = 2 per age) were disaggregated and sorted. For bone marrow, lineage-negative and lineage-positive fractions were collected using a lineage cell depletion kit with an autoMACS Separator (Miltenyi Biotec Inc.) according to the manufacturer's protocol. Stromal and cell components for lymph node, thymus, and spleen were prepared by pressing between frosted glass slides, followed by washing with PBS containing 10% FCS. Splenocytes

were then further analyzed after red blood cell lysis by staining with anti-B220 (Caltag Laboratories Inc.) and anti-CD11b (Mac1; Caltag Laboratories Inc.) mAbs for 30 minutes on ice followed by washing. Cells were sorted by MoFlo (Cytomation Inc.) to B220$^+$, Mac1$^+$, and B220$^-$Mac1$^-$ populations (purity >94%) at the University of North Carolina FACS Core facility.

IHC and SA-β-gal staining. To determine optimal IHC staining conditions for p16^{INK4a}, tissues were harvested from age-matched littermate *p16$^{INK4a+/+}$* and *p16$^{INK4a-/-}$* mice and analyzed. After empiric testing of several fixatives as previously described (62), Fekete's acid alcohol solution (61% ETOH, 4.3% glacial acetic acid, and 3.5% formalin) was determined to be optimal for p16^{INK4a} IHC staining in mouse and rat tissues using a commercially available antibody and kit (ImmunoCruz HRP kit with F-12 antibody, sc-1661; Santa Cruz Biotechnology Inc.). Five-micron paraffin sections were cut and underwent steam citrate antigen retrieval, hybridization per the manufacturer's protocols, and hematoxylin counterstaining. Sections were examined by an observer blinded to animal age, diet, and genotype. SA-β-gal staining was performed as previously described (15, 39, 43). In brief, thin sections (<2 mm) of harvested organs were fixed at room temperature for 15 minutes in 0.5% glutaraldehyde/PBS (pH 6.0). After fixation, organ slices were washed twice in PBS (pH 6.0), stained overnight at 37°C in SA-β-gal buffer (1 mg/ml X-gal, 5 mM potassium ferricyanide, 5 mM potas-sium ferrocyanide, and 1 mM MgCl$_2$ in PBS, pH 6.0), and photographed with a high-resolution CCD camera (LighTools Research).

Address correspondence to: Norman E. Sharpless, The Lineberger Comprehensive Cancer Center, Campus box no. 7295, Departments of Medicine and Genetics, The University of North Carolina School of Medicine, Chapel Hill, North Carolina 27599-7295, USA. Phone: (919) 966-1185, or (919) 966-4067; Fax: (919) 966-8212; E-mail: nes@med.unc.edu.

1. Guarente, L., and Kenyon, C. 2000. Genetic pathways that regulate ageing in model organisms. *Nature.* **408**:255–262.
2. Park, I.K., Morrison, S.J., and Clarke, M.F. 2004. Bmi1, stem cells, and senescence regulation. *J. Clin. Invest.* **113**:175–179. doi:10.1172/JCI200420800.
3. Campisi, J. 2003. Cancer and ageing: rival demons? *Nat. Rev. Cancer.* **3**:339–349.
4. Sharpless, N.E., and DePinho, R.A. 2002. p53: good cop/bad cop. *Cell.* **110**:9–12.
5. Artandi, S.E., et al. 2000. Telomere dysfunction promotes non-reciprocal translocations and epithelial cancers in mice. *Nature.* **406**:641–645.
6. Tyner, S.D., et al. 2002. p53 mutant mice that display early ageing-associated phenotypes. *Nature.* **415**:45–53.
7. Halvorsen, T.L., Beattie, G.M., Lopez, A.D., Hayek, A., and Levine, F. 2000. Accelerated telomere shortening and senescence in human pancreatic islet cells stimulated to divide in vitro. *J. Endocrinol.* **166**:103–109.
8. Alcorta, D.A., et al. 1996. Involvement of the cyclin-dependent kinase inhibitor p16 (INK4a) in replicative senescence of normal human fibroblasts. *Proc. Natl. Acad. Sci. U. S. A.* **93**:13742–13747.
9. Kamijo, T., et al. 1997. Tumor suppression at the mouse INK4a locus mediated by the alternative reading frame product p19ARF. *Cell.* **91**:649–659.
10. Kiyono, T., et al. 1998. Both Rb/p16INK4a inactivation and telomerase activity are required to immortalize human epithelial cells. *Nature.* **396**:84–88.
11. Rheinwald, J.G., et al. 2002. A two-stage, p16(INK4A)- and p53-dependent keratinocyte senescence mechanism that limits replicative potential independent of telomere status. *Mol. Cell. Biol.* **22**:5157–5172.
12. Randle, D.H., Zindy, F., Sherr, C.J., and Roussel, M.F. 2001. Differential effects of p19(Arf) and p16(Ink4a) loss on senescence of murine bone marrow-derived preB cells and macrophages. *Proc. Natl. Acad. Sci. U. S. A.* **98**:9654–9659.
13. Chkhotua, A.B., et al. 2003. Increased expression of p16 and p27 cyclin-dependent kinase inhibitor genes in aging human kidney and chronic allograft nephropathy. *Am. J. Kidney Dis.* **41**:1303–1313.
14. Kajstura, J., et al. 2000. Telomere shortening is an in vivo marker of myocyte replication and aging. *Am. J. Pathol.* **156**:813–819.
15. Melk, A., et al. 2003. Cell senescence in rat kidneys in vivo increases with growth and age despite lack of telomere shortening. *Kidney Int.* **63**:2134–2143.
16. Melk, A., et al. 2004. Expression of p16INK4a and other cell cycle regulator and senescence associated genes in aging human kidney. *Kidney Int.* **65**:510–520.
17. Nielsen, G.P., et al. 1999. Immunohistochemical survey of p16INK4A expression in normal human adult and infant tissues. *Lab Invest.* **79**:1137–1143.
18. Zindy, F., Quelle, D.E., Roussel, M.F., and Sherr, C.J. 1997. Expression of the p16INK4a tumor suppressor versus other INK4 family members during mouse development and aging. *Oncogene.* **15**:203–211.
19. Kanavaros, P., et al. 2001. Immunohistochemical expression of p53, p21/waf1, rb, p16, cyclin D1, p27, Ki67, cyclin A, cyclin B1, bcl2, bax and bak proteins and apoptotic index in normal thymus. *Histol. Histopathol.* **16**:1005–1012.
20. Lessard, J., and Sauvageau, G. 2003. Bmi-1 determines the proliferative capacity of normal and leukaemic stem cells. *Nature.* **423**:255–260.
21. Park, I.K., et al. 2003. Bmi-1 is required for maintenance of adult self-renewing haematopoietic stem cells. *Nature.* **423**:302–305.
22. Molofsky, A.V., et al. 2003. Bmi-1 dependence distinguishes neural stem cell self-renewal from progenitor proliferation. *Nature.* **425**:962–967.
23. Lewis, J.L., et al. 2001. The influence of INK4 proteins on growth and self-renewal kinetics of hematopoietic progenitor cells. *Blood.* **97**:2604–2610.
24. Meng, A., Wang, Y., Van Zant, G., and Zhou, D. 2003. Ionizing radiation and busulfan induce premature senescence in murine bone marrow hematopoietic cells. *Cancer Res.* **63**:5414–5419.
25. Sherr, C.J. 2000. The Pezcoller lecture: cancer cell cycles revisited. *Cancer Res.* **60**:3689–3695.
26. Phelps, D.E., et al. 1998. Coupled transcriptional and translational control of cyclin-dependent kinase inhibitor p18INK4c expression during myogenesis. *Mol. Cell. Biol.* **18**:2334–2343.
27. Pagano, M., et al. 1995. Role of the ubiquitin-proteasome pathway in regulating abundance of the cyclin-dependent kinase inhibitor p27. *Science.* **269**:682–685.
28. Sherr, C.J., and DePinho, R.A. 2000. Cellular senescence: mitotic clock or culture shock? *Cell.* **102**:407–410.
29. Ha, T.U., et al. 2000. Mullerian inhibiting substance inhibits ovarian cell growth through an Rb-independent mechanism. *J. Biol. Chem.* **275**:37101–37109.
30. Ruas, M., and Peters, G. 1998. The p16INK4a/CDKN2A tumor suppressor and its relatives. *Biochim. Biophys. Acta.* **1378**:F115–F177.
31. Uchida, N., and Weissman, I.L. 1992. Searching for hematopoietic stem cells: evidence that Thy-1.1lo Lin- Sca-1+ cells are the only stem cells in C57BL/Ka-Thy-1.1 bone marrow. *J. Exp. Med.* **175**:175–184.
32. Masoro, E.J. 2003. Subfield history: caloric restriction, slowing aging, and extending life. *Sci. Aging Knowledge Environ.* **2003**:RE2.
33. Turturro, A., et al. 1999. Growth curves and survival characteristics of the animals used in the Biomarkers of Aging Program. *J. Gerontol. A Biol. Sci. Med. Sci.* **54**:B492–B501.
34. Yu, B.P., Masoro, E.J., Murata, I., Bertrand, H.A., and Lynd, F.T. 1982. Life span study of SPF Fischer 344 male rats fed ad libitum or restricted diets: longevity, growth, lean body mass and disease. *J. Gerontol.* **37**:130–141.
35. Miller, R.A. 2001. Genetics of increased longevity and retarded aging in mice. In *Handbook of the biology of aging.* E.J. Masoro and S.N. Austad, editors. Academic Press Inc. San Diego, California, USA. 369–395.
36. Bartke, A., et al. 2001. Extending the lifespan of long-lived mice [letter]. *Nature.* **414**:412.
37. Coschigano, K.T., Clemmons, D., Bellush, L.L., and Kopchick, J.J. 2000. Assessment of growth parameters and life span of GHR/BP gene-disrupted mice. *Endocrinology.* **141**:2608–2613.
38. Miller, R.A., et al. 2002. Gene expression patterns in calorically restricted mice: partial overlap with long-lived mutant mice. *Mol. Endocrinol.* **16**:2657–2666.
39. Dimri, G.P., et al. 1995. A biomarker that identifies senescent human cells in culture and in aging skin in vivo. *Proc. Natl. Acad. Sci. U. S. A.* **92**:9363–9367.
40. Ohtani, N., et al. 2001. Opposing effects of Ets and Id proteins on p16INK4a expression during cellular senescence. *Nature.* **409**:1067–1070.
41. Huot, T.J., et al. 2002. Biallelic mutations in p16(INK4a) confer resistance to Ras- and Ets-induced senescence in human diploid fibroblasts. *Mol. Cell. Biol.* **22**:8135–8143.
42. Alani, R.M., Young, A.Z., and Shifflett, C.B. 2001. Id1 regulation of cellular senescence through transcriptional repression of p16/Ink4a. *Proc. Natl. Acad. Sci. U. S. A.* **98**:7812–7816.
43. Jacobs, J.J., Kieboom, K., Marino, S., DePinho, R.A., and van Lohuizen, M. 1999. The oncogene and Polycomb-group gene bmi-1 regulates cell proliferation and senescence through the ink4a locus.

Nature. **397**:164–168.

44. Hara, E., et al. 1996. Regulation of p16CDKN2 expression and its implications for cell immortalization and senescence. *Mol. Cell. Biol.* **16**:859–867.

45. Jacobs, J.J., et al. 2000. Senescence bypass screen identifies TBX2, which represses Cdkn2a (p19(ARF)) and is amplified in a subset of human breast cancers. *Nat. Genet.* **26**:291–299.

46. Palmero, I., Pantoja, C., and Serrano, M. 1998. p19ARF links the tumour suppressor p53 to Ras. *Nature.* **395**:125–126.

47. Serrano, M., et al. 1996. Role of the INK4a locus in tumor suppression and cell mortality. *Cell.* **85**:27–37.

48. Sun, L.Q., et al. 2004. Growth retardation and premature aging phenotypes in mice with disruption of the SNF2-like gene, PASG. *Genes Dev.* **8**:1035–1046.

49. Sharpless, N.E., et al. 2001. Loss of p16Ink4a with retention of p19Arf predisposes mice to tumorigenesis. *Nature.* **413**:86–91.

50. Engwerda, C.R., Handwerger, B.S., and Fox, B.S. 1994. Aged T cells are hyporesponsive to costimulation mediated by CD28. *J. Immunol.* **152**:3740–3747.

51. Yoshimi, N., et al. 1996. Telomerase activity of normal tissues and neoplasms in rat colon carcinogenesis induced by methylazoxymethanol acetate and its difference from that of human colonic tissues. *Mol. Carcinog.* **16**:1–5.

52. Prowse, K.R., and Greider, C.W. 1995. Developmental and tissue-specific regulation of mouse telomerase and telomere length. *Proc. Natl. Acad. Sci. U. S. A.* **92**:4818–4822.

53. Wasylyk, C., Bradford, A.P., Gutierrez-Hartmann, A., and Wasylyk, B. 1997. Conserved mechanisms of Ras regulation of evolutionary related transcription factors, Ets1 and Pointed P2. *Oncogene.* **14**:899–913.

54. Paumelle, R., et al. 2002. Hepatocyte growth factor/scatter factor activates the ETS1 transcription factor by a RAS-RAF-MEK-ERK signaling pathway. *Oncogene.* **21**:2309–2319.

55. Tanaka, K., Oda, N., Iwasaka, C., Abe, M., and Sato, Y. 1998. Induction of Ets-1 in endothelial cells during reendothelialization after denuding injury. *J. Cell. Physiol.* **176**:235–244.

56. Bulavin, D.V., et al. 2004. Inactivation of the Wip1 phosphatase inhibits mammary tumorigenesis through p38 MAPK-mediated activation of the p16(Ink4a)-p19(Arf) pathway. *Nat. Genet.* **36**:343–350.

57. Leung, C., et al. 2004. Bmi1 is essential for cerebellar development and is overexpressed in human medulloblastomas. *Nature.* **428**:337–341.

58. Gil, J., Bernard, D., Martinez, D., and Beach, D. 2004. Polycomb CBX7 has a unifying role in cellular lifespan. *Nat. Cell Biol.* **6**:67–72.

59. Kranc, K.R., et al. 2003. Transcriptional coactivator Cited2 induces Bmi1 and Mel18 and controls fibroblast proliferation via Ink4a/ARF. *Mol. Cell. Biol.* **23**:7658–7666.

60. Brunet, A., et al. 2004. Stress-dependent regulation of FOXO transcription factors by the SIRT1 deacetylase. *Science.* **303**:2011–2015.

61. Cohen, H.Y., et al. 2004. Calorie restriction promotes mammalian cell survival by inducing the SIRT1 deacetylase. *Science.* **305**:390–392.

62. Mikaelian, I., et al. 2004. Antibodies that label paraffin-embedded mouse tissues: a collaborative endeavor. *Toxicol. Pathol.* **32**:181–191.

63. Chimenti, C., et al. 2003. Senescence and death of primitive cells and myocytes lead to premature cardiac aging and heart failure. *Circ. Res.* **93**:604–613.